Eur. Phys. J. E (2014) **37**: 106
DOI 10.1140/epje/i2014-14106-2

THE EUROPEAN PHYSICAL JOURNAL E

Regular Article

Thermodiffusion, molecular diffusion and Soret coefficient of binary and ternary mixtures of n-hexane, n-dodecane and toluene*

David Alonso de Mezquia[1], Zilin Wang[2], Estela Lapeira[1], Michael Klein[2], Simone Wiegand[2,3,a], and M. Mounir Bou-Ali[1,b]

[1] Manufacturing Department, MGEP Mondragon Goi Eskola Politeknikoa, Loramendi 4 Apartado 23, 20500 Mondragon, Spain
[2] Research Center Jülich, ICS-3 - Soft Condensed Matter, D-52428 Jülich, Germany
[3] Chemistry Department - Physical Chemistry, University Cologne, 50939 Cologne, Germany

Received 22 June 2014 and Received in final form 11 September 2014
Published online: 10 November 2014 –

Abstract. In this study, the thermodiffusion, molecular diffusion, and Soret coefficients of 12 binary mixtures composed of toluene, *n*-hexane and *n*-dodecane in the whole range of concentrations at atmospheric pressure and temperatures of 298.15 K and 308.15 K have been determined. The experimental measurements have been carried out using the Thermogravitational Column, the Sliding Symmetric Tubes and the Thermal Diffusion Forced Rayleigh Scattering techniques. The results obtained using the different techniques show a maximum deviation of 9% for the thermodiffusion coefficient, 8% for the molecular diffusion coefficient and 2% for the Soret coefficient. For the first time we report a decrease of the thermodiffusion coefficient with increasing ratio of the thermal expansion coefficient and viscosity for a binary mixture of an organic ring compound with a short *n*-alkane. This observation is discussed in terms of interactions between the different components. Additionally, the thermogravitational technique has been used to measure the thermodiffusion coefficients of four ternary mixtures consisting of toluene, *n*-hexane and *n*-dodecane at 298.15 K. In order to complete the study, the values obtained for the molecular diffusion coefficient in binary mixtures, and the thermodiffusion coefficient of binary and ternary mixtures have been compared with recently derived correlations.

1 Introduction

A temperature gradient within a liquid mixture generates mass fluxes that tend to separate its components. This effect at the same time generates fluxes in the opposite direction due to molecular diffusion. This phenomenon is known as thermodiffusion or Ludwig-Soret effect [1, 2]. The flux (J) for one of the components of the mixture (i) generated by this effect can be described using the following expression:

$$J_i = -\rho \left(\sum_{k=1}^{n-1} D_{ik} \nabla c_k + D_{\mathrm{T}}^{i} \nabla T \right), \quad i = 1, 2, \ldots, (n-1), \tag{1}$$

where ρ is the density of the mixture, c_k is the mass fraction of component k, ∇T is the applied temperature gradient, D_{ik} is the molecular Fick diffusion coefficient and D_{T}^{i} is the thermodiffusion coefficient of the i component. In this equation n refers to the number of components of the mixture. This phenomenon is of particular importance in several fields, such as solar ponds [3–5], geologic processes [6–8] or separation processes in liquids [9]. Furthermore, it has aroused interest in petroleum industry [10–12] and it is also used in biotechnology [13, 14].

Numerous former studies of binary mixtures have reported that parameters, such as molar mass, size and shape have significant impact on the thermodiffusion process, however, in liquid mixtures of non-polar molecules, physical properties like thermal expansion, moment of inertia and polarity show particular importance [15–17], while in aqueous mixtures and solutions structural changes such as breakdown of the hydrogen bond network are more important [18–20]. Already in 2006, an elementary theory predicted a linear correlation between the thermodiffusion coefficient and the ratio of thermal expansion coefficient to kinematic viscosity [21]. Later, this theory was confirmed experimentally in both organic [22] and aqueous systems [23].

* Contribution to the Topical Issue "Thermal non-equilibrium phenomena in multi-component fluids" edited by Fabrizio Croccolo and Henri Bataller.

[a] e-mail: s.wiegand@fz-juelich.de
[b] e-mail: mbouali@mondragon.edu

Table 1. Mass fraction of each component in the ternary mixtures and their corresponding binary mixtures.

Mixture	Component mass fraction		
	toluene (Tol)	n-dodecane (nC_{12})	n-hexane (nC_6)
I	0.2642	0.4885	0.2471
I.1	0.5167	0	0.4832
I.2	0.3510	0.6489	0
I.3	0	0.6640	0.3359
II	0.2413	0.6218	0.1367
II.1	0.6405	0	0.3594
II.2	0.2787	0.7212	0
II.3	0	0.8218	0.1781
III	0.2920	0.3272	0.3807
III.1	0.4331	0	0.5668
III.2	0.4741	0.5258	0
III.3	0	0.4586	0.5413
IV	0.3333	0.3333	0.3333
IV.1	0.5000	0	0.5000
IV.2	0.5000	0.5000	0
IV.3	0	0.5000	0.5000

There are many studies, both theoretical and experimental, about thermodiffusion in binary mixtures [15,24–31], but in most technical processes we have to deal with multicomponent mixtures and not only with binary mixtures [32]. Although much effort has been made in the theoretical treatment of multicomponent mixtures [33,34], only a few ternary mixtures have been experimentally investigated [35–40]. In this sense ternary mixtures are of particular importance when going from binary to multicomponent mixtures. They show more characteristic features of true multicomponent systems than binary mixtures, such as cross and reverse diffusion. Meanwhile, they are still experimentally accessible.

In this work, four ternary mixtures consisting of toluene, n-dodecane and n-hexane and their corresponding binary mixtures will be analyzed. The corresponding binary mixtures are the ones that maintain the same mass concentration of two of the components in the ternary mixtures but in a binary mixture. The ternary mixtures will be studied at a mean temperature of 298.15 K while the binary mixtures will be studied at both 298.15 K and 308.15 K. The measurements in binary mixtures will be carried out using three different techniques. The results obtained from the Thermogravitational Column (TGC) and the Sliding Symmetric Tubes (SST) techniques will be compared with the data from Thermal Diffusion Forced Rayleigh Scattering (TDFRS). Ternary mixtures will be investigated only with the Thermogravitational Column technique. The mass fraction of each component in the studied ternary mixtures and in the corresponding binary mixtures are listed in table 1.

The measured thermodiffusion coefficients have been compared with values predicted by two correlations developed in previous TGC studies [35, 41, 42]. In the case of binary mixtures, the obtained experimental results for the mixtures of n-hexane and n-dodecane will be compared with the correlation found earlier [41]. In the case of ternary mixtures the correlation by Blanco *et al.* [35] will be used for comparison. In a similar way, the values obtained for the molecular diffusion coefficient for the mixture n-dodecane/n-hexane have been compared with the ones obtained using the correlations developed by Alonso de Mezquia *et al.* [42] and Madariaga *et al.* [41]. These correlations have been used only for the mixtures of n-hexane and n-dodecane as these correlations have been developed and validated only for binary n-alkane mixtures.

The paper is organized as follows. In experimental section the techniques used (TGC, SST and TDFRS) and the different experimental procedures used for the determination of the properties of the studied binary and ternary mixtures will be explained. In the first part of results section the thermodiffusion coefficient, D_T, the molecular diffusion coefficient, D, and the Soret coefficient, S_T, obtained in the binary mixtures using the different techniques are given and discussed. In the second part of this section, the results obtained for the ternary mixtures are presented. In the last section the results are summarized.

2 Experimental section

2.1 Sample preparation

2.1.1 Thermogravitational columns and Sliding Symmetric Tubes

All the products used in the experiments carried out in the TGC and SST devices have been purchased from Merck, with a purity better than 99%. The mixtures have been prepared by weight, adding first the less volatile compound, and later on the second component until the desired concentration is obtained. When preparing the mixtures two high accuracy digital scales have been used. One of the scales has a capacity up to 4500 g and an accuracy of 0.01 g. This one has been used for the preparation of the mixtures used in the cylindric thermogravitational column, in which a quantity of 230 cm^3 of fluid is needed to carry out a measurement. The second digital scale has a capacity of 310 g and an accuracy of 0.0001 g. This one has been used in the preparation of the mixtures used in the parallelepiped thermogravitational column and for the determination of the density, viscosity, thermal and mass expansion coefficients, and for the calibration procedure. The relative uncertainty on sample preparation is lower than $3 \cdot 10^{-5}$.

2.1.2 TDFRS

All the chemicals were purchased from Sigma-Aldrich with analytical purity (Guaranteed Reagent) and were used

without further purification. The TDFRS experiments require a small amount of dye in the sample. In this work, all samples contained approximately 0.002 wt% of the dye quinizarin (Aldrich). This amount ensures a sufficient optical modulation of the grating but is small enough to avoid contributions of the dye to the concentration signal. Before each TDFRS experiment, approximately 2 cm^3 of the freshly prepared solution was filtered through a 0.2 μm filter (hydrophobic polytetrafluoroethylene) into a quartz cell with 0.2 mm optical path length (Helma®) which was carefully cleaned from dust particles before usage.

After each measurement we checked carefully the meniscus height in the two filling capillaries of the sample cell in order to detect whether the volatile solvent evaporated during the measurement. The accuracy of this method is certainly better than 1%. The total volume of the sample cell is in the order of 0.6 cm^3. Typically the experimental uncertainties for S_T, D_T and D are below 5, 8 and 7%, respectively.

2.2 Data analysis and setup

2.2.1 Thermogravitational columns

In this study, for the determination of the thermodiffusion coefficient, two different thermogravitational columns have been used. One has a parallelepiped configuration and the other one has a cylindrical configuration. A complete description of both columns can be seen elsewhere [35].

According to F.J.O. theory [43], the stationary separation of the components in a thermogravitational column in the case of a ternary mixture can be related to the thermodiffusion coefficient, $\mathbf{D}_T$, of component i by the following expression:

$$\frac{\partial c_i}{\partial z} = -\frac{504}{gL_x^4}\frac{\mathbf{D}_T^i \nu}{\alpha} \quad i = 1, 2, \ldots, (1-n), \tag{2}$$

where $\alpha = -(1/\rho)(\partial\rho/\partial T)$ is the thermal expansion coefficient, ν the kinematic viscosity, g is the gravitational acceleration, L_z is the height of the column (500 mm) and L_x is the gap between the hot and cold wall (1.000 ± 0.005 mm). More details are described in another paper [35].

When working with binary mixtures, the thermodiffusion coefficient can be defined as $\mathbf{D}_T^i = c_i c_j D_T^i$. Additionally, one can introduce the mass expansion coefficient $\beta_i = (1/\rho)(\partial\rho/\partial c_i)$ of the mixture, so that the thermodiffusion coefficient in binary mixtures can be obtained by means of eq. (3) [25]

$$D_T^i = -\frac{gL_x^4}{504}\frac{\alpha}{c_i c_j \beta_i \rho \nu}\frac{\partial \rho}{\partial z}. \tag{3}$$

In order to obtain the concentration variation $(\partial c_i/\partial z)$ along the column, a calibration has to be done. It is used to obtain the concentration of each component in the mixture from the data of the density, in the case of binary mixtures, and density and refractive index in the case of the ternary mixtures [38]. When using this technique, the uncertainty in the determination of the thermodiffusion coefficient in binary mixtures is around 5%. In the case of ternary mixtures, as the separation of the components inside the column is smaller, this factor increases to around 10%.

2.2.2 Sliding Symmetric Tubes

The Sliding Symmetric Tubes technique [42] consists of several sets with two identical vertical tubes. The studied mixture, with a slight mass fraction difference ($c_0 \pm 3\%$), is introduced in these tubes. The sets are then introduced in a water bath so that the mixture equilibrates at the measurement temperature. Analyzing the change of concentration in the tubes as a function of time, the molecular diffusion coefficient of the mixture can be obtained. In the case of binary mixtures D is determined by

$$\overline{c^{\mathrm{up}}}(t) - \frac{c_i^{\mathrm{up}} + c_i^{\mathrm{bot}}}{2} = \frac{8}{\pi^2}\left(c_i^{\mathrm{up}} - \frac{c_i^{\mathrm{up}} + c_i^{\mathrm{bot}}}{2}\right)\Phi, \tag{4}$$

$$\overline{c^{\mathrm{bot}}}(t) - \frac{c_i^{\mathrm{up}} + c_i^{\mathrm{bot}}}{2} = -\frac{8}{\pi^2}\left(c_i^{\mathrm{up}} - \frac{c_i^{\mathrm{up}} + c_i^{\mathrm{bot}}}{2}\right)\Phi, \tag{5}$$

where

$$\Phi = \sum_{n=0}^{\infty} \frac{e^{-\left(n+\frac{1}{2}\right)^2 \frac{\pi^2}{L^2} Dt}}{(2n+1)^2}. \tag{6}$$

$\overline{c^{\mathrm{up/bot}}}(t)$ is the mean concentration of the denser component in the upper and bottom tube, respectively, $c_i^{\mathrm{up/bot}}$ is the initial concentration of the denser component in the tubes, L is the length of the each tube (half of the diffusion path), t is the time of experiment and D is the molecular diffusion coefficient. Taking into account the experimental procedure, the uncertainty in the determination of the molecular diffusion coefficient with this technique is around 3% [44].

2.2.3 TDFRS

The TDFRS setup has been described in detail before [45]. A holographic grating is formed by a solid state laser ($\lambda_w = 488$ nm) for writing and is read out by a He-Ne laser ($\lambda_r = 633$ nm). By adding a small amount of quinizarin, the blue light grating is converted into a temperature grating. The induced concentration grating is read out by the He-Ne laser and the normalized heterodyne scattering intensity $\zeta_{\mathrm{het}}(t)$, assuming an ideal excitation with a step function, is given by

$$\zeta_{\mathrm{het}}(t) = 1 - \exp\left(-\frac{t}{\tau_{\mathrm{th}}}\right) - A(\tau - \tau_{\mathrm{th}})^{-1} \times \left\{\tau\left[1 - \exp\left(-\frac{t}{\tau}\right)\right] - \tau_{\mathrm{th}}\left[1 - \exp\left(-\frac{t}{\tau_{\mathrm{th}}}\right)\right]\right\},$$

Table 2. Thermophysical properties at 298.15 K and different mass fractions of the studied binary mixtures.

Mixture	c_1	ρ/kg m^{-3}	$\alpha/10^{-3}$ K^{-1}	β	$\mu/10^{-3}$ Pa s	$\left(\frac{\partial n}{\partial c}\right)_{p,T}$	$\left(\frac{\partial n}{\partial T}\right)_{P,c}/10^{-4}$ K^{-1}
Tol-nC$_6$	0.053	663.583	1.369	0.2430	0.3237	-	-
”	0.2630	699.368	1.305	0.2572	0.3443	-	-
”	0.4331	731.425	1.255	0.2679	0.3693	0.1210[a]	−5.4800
”	0.5000	744.757	1.231	0.2734	0.3852	0.1210[a]	−5.4800
”	0.5167	748.213	1.230	0.2754	0.3855	0.1210[a]	−5.4900
”	0.6405	774.495	1.200	0.2839	0.4164	0.1210[a]	−5.5000
Tol-nC$_{12}$	0.2787	772.611	1.000	0.1348	0.9485	0.0691[b]	−4.6300
”	0.3510	780.306	1.008	0.1406	0.8814	0.0691[b]	−4.6600
”	0.4741	793.966	1.022	0.1438	0.7861	0.0691[b]	−4.8900
”	0.5000	796.902	1.023	0.1450	0.7690	0.0691[b]	−4.9000
nC$_{12}$-nC$_6$	0.4586	695.112	1.174	0.1288	0.5244	0.0471[c]	−4.8318
”	0.5000	698.780	1.158	0.1282	0.5636	0.0471[c]	−4.7869
”	0.6640	713.777	1.094	0.1289	0.7115	0.0471[c]	−4.6120
”	0.8218	728.268	1.035	0.1288	0.9401	0.0471[c]	−4.4955

[a] Deviation = 1.62×10^{-3}.
[b] Deviation = 6.33×10^{-4}.
[c] Deviation = 3.46×10^{-4}.

with the steady state amplitude A

$$A = \left(\frac{\partial n}{\partial c}\right)_{p,T} \left(\frac{\partial n}{\partial T}\right)_{p,c}^{-1} S_{\mathrm{T}} c(1-c), \qquad (7)$$

where c is the mass fraction, τ_{th} the heat diffusion time, τ the equilibration time for the mass diffusion, S_{T}, the Soret coefficient, $(\partial n/\partial c)_{p,T}$ and $(\partial n/\partial T)_{p,c}$ are refractive index contrast factors with respect to mass fraction at constant pressure and temperature, and temperature at constant pressure and mass fraction, respectively. The equilibration time for the temperature grating τ_{th} can be used to calculate the thermal diffusivity, $D_{\mathrm{th}} = \kappa/\rho c_p$, which describes the heat transport in the solution, and corresponds to the ratio of the thermal conductivity, κ, over the product of density, ρ, and specific heat capacity at constant pressure, c_p. The collective diffusion coefficient, $D = \tau q^2$, can be determined from the time constant for the mass diffusion, τ and the grating vector, $q = (4\pi/\lambda_w)\sin\theta/2$ with θ the scattering angle between the two blue writing beams.

2.2.4 Density measurements

The density measurements have been performed by an Anton Paar DMA 5000 vibrating tube density meter, having a resolution of $1 \cdot 10^{-6}$ g cm^{-3} and a temperature accuracy of 0.001 K using only 1.5 cm^3 of sample for the measurements. The relative uncertainty on density measurements is around $5 \cdot 10^{-6}$.

2.2.5 Refractive index measurements

An Anton Paar RXA 156 refractometer has been used to measure the refractive index of the mixtures as well as to determine the increments with the mass fraction $(\partial n/\partial c)_{p,T}$. It has a repeatability of $2 \cdot 10^{-5}$, and the temperature accuracy is ±0.01 K. The volume needed to make one measurement is less than 1 cm^3. For all investigated temperatures and concentrations we find a linear dependence of the refractive index on concentration if the temperature is fixed or on temperature if the concentration is fixed. For all mixtures we determined the $(\partial n/\partial c)_{p,T}$ values. The refractometer uses the sodium line with a wavelength of 589.3 nm, which is roughly 40 nm shorter than the HeNe-laser of 632.8 nm used as read-out beam in the TDFRS technique. This causes a small systematic error in the refractive index increment in the order of 0.5–1% [46,47].

2.2.6 Viscosity measurements

The dynamic viscosity of the mixtures has been determined by an Anton Paar AMVn falling ball microviscometer which has a reproductivity in its measurements of over 99%. The temperature is controlled by a Peltier system which gives a temperature stability of ±0.01 K.

Tables 2 and 3 show the measured density, ρ, thermal expansion coefficient, α, mass expansion coefficient, β, dynamic viscosity, μ, and contrast factors, $(\partial n/\partial c)_{p,T}$ and $(\partial n/\partial T)_{P,c}$, of the studied binary mixtures at different concentrations at both 298.15 K and 308.15 K temperatures, while in table 4 the data obtained for the density, ρ, thermal expansion coefficient, α, and dynamic viscosity, μ, for the ternary mixtures at 298.15 K can be seen. The values of density and viscosity of mixtures are compared with available literature values and they agree within 1.7% and 6.5%, respectively [48–51].

Table 3. Thermophysical properties at 308.15 K and different mass fractions of the studied binary mixtures.

Mixture	c_1	ρ/kg m^{-3}	$\alpha/10^{-3}$ K^{-1}	$\mu/10^{-3}$ Pa s	$\left(\frac{\partial n}{\partial c}\right)_{p,T}$	$\left(\frac{\partial n}{\partial T}\right)_{P,c}/10^{-4}$ K^{-1}
Tol-nC$_6$	0.053	654.407	1.415	0.2979	-	-
”	0.2630	690.160	1.345	0.3158	-	-
”	0.4331	722.131	1.287	0.3373	0.1205[a]	−5.5400
”	0.5000	735.573	1.260	0.3521	0.1205[a]	−5.5400
”	0.5167	735.944	1.256	0.3525	0.1205[a]	−5.5500
”	0.6405	765.235	1.216	0.3782	0.1205[a]	−5.5700
Tol-nC$_{12}$	0.2787	764.853	1.017	0.8370	0.0676[b]	−4.5800
”	0.3510	772.411	1.024	0.7653	0.0676[b]	−4.6600
”	0.4741	785.827	1.038	0.6862	0.0676[b]	−4.8200
”	0.5000	788.715	1.040	0.6738	0.0676[b]	−4.8800
nC$_{12}$-nC$_6$	0.4586	686.825	1.203	0.4657	0.0480[c]	−4.9042
”	0.5000	690.604	1.185	0.4959	0.0480[c]	−4.8704
”	0.6640	706.090	1.113	0.6218	0.0480[c]	−4.6661
”	0.8218	720.818	1.090	0.8059	0.0480[c]	−4.5180

[a] Deviation $= 1.63 \times 10^{-3}$.
[b] Deviation $= 7.16 \times 10^{-4}$.
[c] Deviation $= 7.72 \times 10^{-4}$.

Table 4. Thermophysical properties of the ternary mixtures of the components Tol-nC$_{12}$-nC$_6$ at 298.15 K and different mass fractions.

Mixture	c_1	c_2	c_3	ρ/kg m^{-3}	$\alpha/10^{-3}$ K^{-1}	$\mu/10^{-3}$ Pa s
Tol-nC$_{12}$-nC$_6$	0.2642	0.2471	0.4885	754.713	1.047	0.7527
”	0.2413	0.6218	0.1367	746.337	1.091	0.6240
”	0.2920	0.3272	0.3807	736.305	1.151	0.5130
”	0.3333	0.3333	0.3333	744.643	1.137	0.5241

3 Results and discussion

3.1 Binary mixtures

3.1.1 Thermodiffusion coefficient

In table 5 the results obtained for the thermodiffusion coefficient at 298.15 K and 308.15 K by the Thermal Diffusion Forced Rayleigh Scattering (TDFRS) and the thermogravitational column (TGC) are shown. In the case of the thermogravitational technique the value of the thermodiffusion coefficient shown is the mean value of the coefficients measured with both columns (parallelepiped and cylindric one). Additionally, in the normal alkane mixtures, the results obtained using the correlation developed by Madariaga *et al.* [41] are presented.

As can be seen in table 5, there exist differences between the values obtained with both techniques and the ones calculated with the correlation [41]. On average the deviations between the measurements with TGC and TDFRS are about 3% and the maximum deviation is 8.5%. In table 1 the experimental thermodiffusion coefficients of the Tol-nC$_6$ mixture obtained in this work are compared with literature values [52, 53]. It can be seen that the data are in good agreement within the experimental errors. Especially at 298.15 K, the lower temperature, the deviations between two experimental techniques are typically below 1.1%. At 308.15 K the typical deviations are below 2%. Compared with the literature value for the equimolar mixture at 298.15 K [54] with deviations between 2 and 3% for TGC and TDFRS data, respectively. In fig. 1 we also included the thermal diffusion coefficients measured by Zhang *et al.* [55]. Please note that the data given in table 5 of the mentioned paper are accidently given as function of the n-hexane mass (mole) fraction, while the figures show the correct values as function of the toluene concentration. The deviations from the other data are well below 9%. The obtained data show an increase of the thermodiffusion coefficient with increasing temperature. This can be understood due to a higher mobility of the molecules as consequence of the decreasing viscosity at higher temperature. This behavior is in agreement with previous studies [54].

According to Brenner [21], the thermodiffusion coefficient, D_T, of dilute solutions shows a linear correlation with the thermal expansion coefficient α and the diffusion coefficient D. As D is inversely proportional to the

Table 5. Results of the Thermodiffusion Coefficient Using the TDFRS and the Thermogravitational Techniques for the Mixtures Tol-nC$_6$, Tol-nC$_{12}$ and nC$_{12}$-nC$_6$ and the Ones Obtained Using the Correlation by Madariaga *et al.* [41] for nC$_{12}$-nC$_6$ Mixture Both at 298.15 K and 308.15 K. δ is the Deviation Between the TDFRS and TGC Measurements.

Mixture	c_1	$D_T/10^{-12}$ m^2 s^{-1} K^{-1}							
		298.15 K				308.15 K			
		TDFRS	TGC	δ/%	Corr. [41]	TDFRS	TGC	δ/%	Corr. [41]
Tol-nC$_6$	0.053	-	12.80	-	-	-	13.08	-	-
”	0.2630	-	12.77	-	-	-	13.71	-	-
”	0.4331	13.30	13.38	0.6	-	14.09	14.36	1.9	-
”	0.5000	13.56	13.51	0.3	-	14.68	14.44	1.7	-
”	0.5167	13.73	13.70	0.2	-	14.79	14.79	1.4	-
”	0.6405	13.94	14.09	1.1	-	14.65	14.82	1.1	-
Tol-nC$_{12}$	0.2787	2.00	1.95	2.3	-	2.54	2.41	5.2	-
”	0.3510	2.55	2.38	7.0	-	3.09	2.88	7.0	-
”	0.4741	3.40	3.14	8.1	-	3.97	3.64	8.6	-
”	0.5000	3.37	3.39	0.5	-	3.96	3.87	2.2	-
nC$_{12}$-nC$_6$	0.4586	7.95	8.02	0.8	7.72	8.54	8.46	1.0	8.91
”	0.5000	7.24	7.67	5.7	7.38	8.26	7.97	3.6	8.58
”	0.6640	6.55	6.69	2.1	6.54	6.76	7.12	5.2	7.61
”	0.8218	5.32	5.79	8.5	5.53	6.36	6.61	3.9	6.80

Table 6. Results for the molecular diffusion coefficient using the TDFRS technique for Tol-nC$_6$, Tol-nC$_{12}$ and nC$_{12}$-nC$_6$ mixtures and the ones obtained for nC$_{12}$-nC$_6$ mixture using the SST technique and the correlation by Alonso de Mezquia *et al.* [42] at 298.15 K and 308.15 K.

Mixture	c_1	$D/10^{-9}$ m^2 s^{-1}				
		298.15 K			308.15 K	
		TDFRS	SST	Corr. [42]	TDFRS	Corr. [42]
Tol-nC$_6$	0.4331	3.04	-	-	3.63	-
”	0.5000	2.91	-	-	3.34	-
”	0.5167	2.85	-	-	3.29	-
”	0.6405	2.49	-	-	2.80	-
Tol-nC$_{12}$	0.2787	1.49	-	-	1.89	-
”	0.3510	1.56	-	-	1.91	-
”	0.4741	1.49	-	-	1.81	-
”	0.5000	1.47	-	-	1.75	-
nC$_{12}$-nC$_6$	0.4586	2.24	2.26	2.15	2.51	2.44
”	0.5000	2.06	2.13	2.09	2.39	2.38
”	0.6640	1.94	1.93	1.87	2.03	2.12
”	0.8218	1.59	1.73	1.65	1.99	1.88

kinematic viscosity ν, it holds $D_T \propto \alpha/\nu$. In most previous studies for non-polar [22] and even for polar systems [23, 56] a linear increase of D_T as function of α/ν has been observed experimentally. Figure 2(a), (b) and (c) display D_T of toluene-nC$_6$, toluene-nC$_{12}$, nC$_{12}$-nC$_6$ as function of α/ν. The thermodiffusion coefficients of toluene-nC$_{12}$ and nC$_{12}$-nC$_6$ increase linearly, but D_T of toluene-nC$_6$ decreases as function of α/ν. As the thermal expansion coefficient of the toluene-nC$_6$ mixture decreases and the viscosity of the mixture increases with increasing toluene content, it means that D_T of toluene-nC$_6$ increases with increasing toluene content. To our best knowledge the only other systems in the literature showing a similar decrease of D_T with α/ν are benzene-nC$_6$ and benzene-nC$_7$ [57] shown in fig. 2(d). Note that benzene has a similar chemical ring structure as toluene. While an increase of D_T as function α/ν seems to be physical intuitive, because a lower viscosity leads to a faster diffusion and a higher sensitivity to temperature changes should also lead to an increasing thermodiffusion, the opposite trend seems to be rather counter intuitive. In order to gain some understanding we regard the interaction energies of the mixtures. For a pure solvent with low intra-molecular interactions we expect a larger thermal

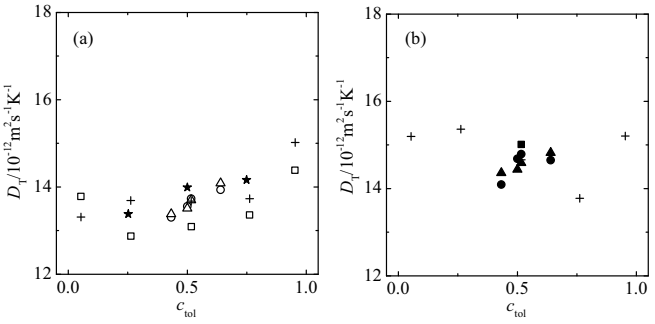

Fig. 1. D_T of the mixture Tol-nC$_6$ as function of mass fraction of toluene. (a) Open symbols mark the D_T-values at 298.15 K and (b) solid symbols at 308.15 K. The TDFRS and TGC measurements are marked by a circle and triangle, respectively. The values from the literature [52–55] are presented by square, star, solid square and cross symbols, respectively.

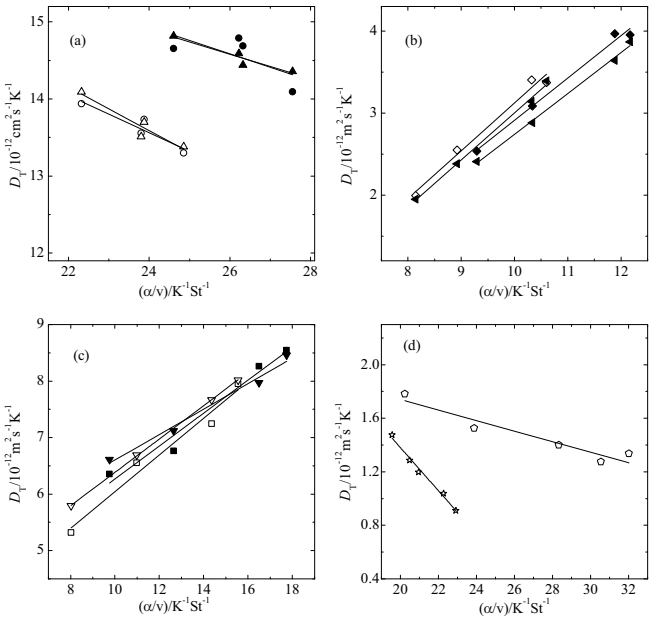

Fig. 2. D_T of the three mixtures as function of the ratio of the thermal expansion coefficient, α, and the kinematic viscosity, ν. (a) toluene-nC$_6$ (TDFRS ○, ●, TGC △, ▲), (b) toluene-nC$_{12}$ (TDFRS ◇, ◆, TGC ◁, ◀), (c) nC$_{12}$-nC$_6$ (TDFRS □, ■, TGC ▽, ▼), (d) benzene-nC$_6$ (☆) and benzene-nC$_7$ (⬠) from literature data [57]. All the open symbols present the results of measurements at 298.15 K and solid symbols are at 308.15 K. The lines correspond to linear fits of the data points.

expansion coefficient than for solvents with strong molecular interactions. In the case of solvent mixtures we expect a larger separation if the cross interactions (between different molecules) are weaker than the intra-molecular interaction (between the same molecules). A recent two-chamber lattice model gives a good qualitative description of the thermodiffusion behavior of benzene-alkane mixtures [16]. It turns out that benzene-benzene interactions are stronger than the heptane-heptane and the benzene-heptane interactions. Therefore, addition of benzene leads

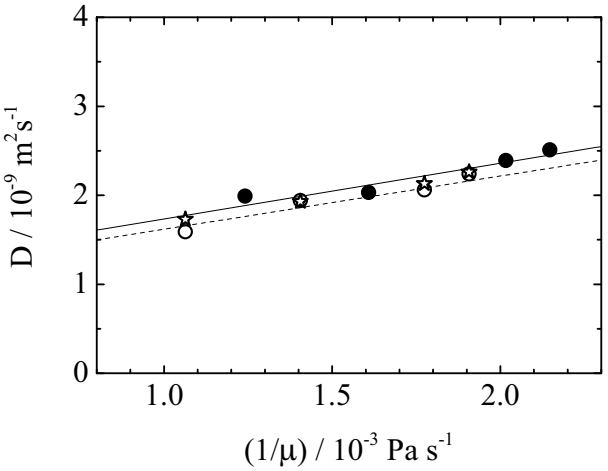

Fig. 3. Values for the molecular diffusion coefficient, D, for the mixture nC$_{12}$-nC$_6$ studied at 298.15 K (TDFRS ○, SST ☆) and 308.15 K (TDFRS ●) as function of the inverse of the dynamic viscosity, μ, of the mixtures. The dashed and solid lines correspond to the correlation given by Alonso de Mezquia *et al.* [42] at 298.15 K and 308.15 K, respectively.

to an easier separation from heptane, *i.e.* an increasing D_T. As in the case of toluene-nC$_6$ the thermal expansion coefficient of benzene-nC$_6$ decreases and the viscosity increases with increasing benzene content. These two observations lead to the unusual decrease of D_T with α/ν. With increasing chain length of the n-alkanes the intramolecular interactions of the n-alkanes and cross interaction between benzene and n-alkane increase [16], so that D_T will no longer increase with increasing concentration of the organic ring compound. Therefore above a certain chain length the dependence of D_T on α/ν will be reversed. Due to the similar chemical structure of toluene and benzene it is reasonable to assume the same behavior for toluene. Our hypothesis for the chain length dependence is supported by the fact that D_T of toluene-nC$_{12}$ shows the reversed trend. Note that Brenner's theory is only valid for dilute solutions, which might be the reason for the benzene-hexane mixture to be deviated from the linear fit and to seem to show a minimum of D_T.

3.1.2 Molecular diffusion coefficient

Table 6 shows the values for the molecular diffusion coefficient for the studied mixtures measured with the TDFRS technique and the SST technique. Additionally, the ones obtained with the correlation developed by Alonso de Mezquia *et al.* [42] are listed. The data obtained for the molecular diffusion coefficient with the two techniques can only be compared for four of the mixtures. The largest deviation between data from TDFRS and correlation is 4.3%, while deviation between SST and correlation is 5.0%. The maximum deviation of 8.2% between data from TDFRS and SST appears for the sample with high dodecane concentration. As expected from the Stokes-Einstein

Table 7. Results obtained of the Soret coefficient using the TDFRS technique for Tol-nC$_6$, Tol-nC$_{12}$ and nC$_{12}$-nC$_6$ mixtures and the combination of SST and TGC techniques for nC$_{12}$-nC$_6$ mixture at 298.15 K and 308.15 K.

Mixture	c_1	$S_T/10^{-3}\,K^{-1}$ 298.15 K		308.15 K
		TDFRS	SST-TGC	TDFRS
Tol-nC$_6$	0.4331	4.37	-	3.88
”	0.5000	4.66	-	4.39
”	0.5167	4.82	-	4.49
”	0.6405	5.59	-	5.23
Tol-nC$_{12}$	0.2787	1.34	-	1.34
”	0.3510	1.64	-	1.61
”	0.4741	2.29	-	2.19
”	0.5000	2.29	-	2.27
nC$_{12}$-nC$_6$	0.4586	3.54	3.54	3.40
”	0.5000	3.51	3.60	3.46
”	0.6640	3.39	3.46	3.33
”	0.8218	3.34	3.34	3.19

relation the molecular diffusion coefficient of the mixture nC$_{12}$-nC$_6$ increases linearly with the inverse of the dynamic viscosity (cf. fig. 3). The data obtained has been also compared with the data found in the literature [55] and in all the cases the differences have been within the experimental error.

3.1.3 Soret coefficient

Table 7 lists the results for the Soret coefficient of the studied mixtures. This table includes the results obtained by direct measurements for Tol-nC$_6$, Tol-nC$_{12}$ and nC$_{12}$-nC$_6$ mixtures using the TDFRS and the calculated values for the nC$_{12}$-nC$_6$ mixture. The calculated S_T values have been determined using the thermodiffusion coefficient measured by the TGC and the molecular diffusion coefficient measured by the SST technique. In this case the error in the Soret coefficients given in the tables is around 8%.

The Soret coefficient of the studied mixtures decreases when the temperature rises. The reason is that the temperature influence on the diffusion coefficient is stronger than that on the thermodiffusion coefficient. The same trend has been observed for equimolar toluene and n-hexane mixtures [54].

Figure 4 summarizes the results determined with the TDFRS, SST and TGC for the Soret coefficient, the thermodiffusion coefficient and the molecular diffusion coefficient for the mixture nC$_6$-nC$_{12}$ at 298.15 K and 308.15 K. All three coefficients decrease with increasing concentration of nC$_{12}$.

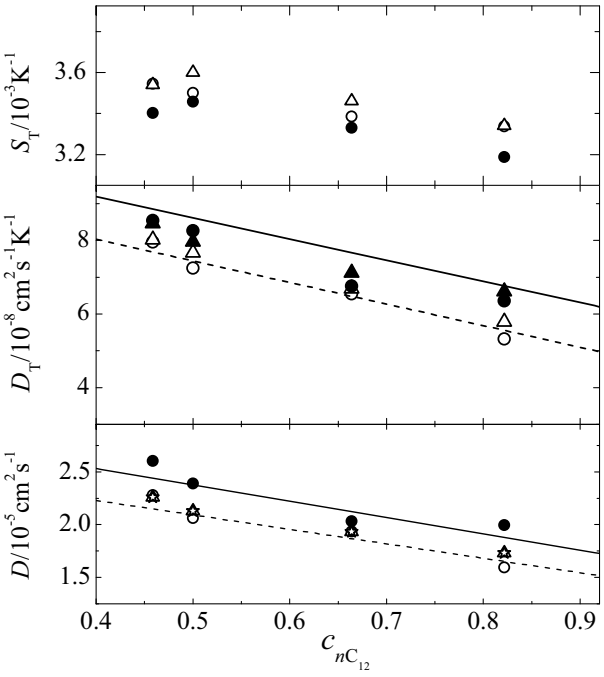

Fig. 4. Values for the Soret coefficient, thermodiffusion coefficient and molecular diffusion coefficient for the mixture nC$_{12}$-nC$_6$ studied at 298.15 K (open symbols) and 308.15 K (solid symbols) obtained using the TDFRS (○, ●), TGC (△, ▲) and SST (☆) techniques as function of the mass fraction of nC$_{12}$.

3.2 Ternary mixtures

3.2.1 Thermodiffusion coefficient

The obtained results for the thermodiffusion coefficient of the four ternary mixtures studied can be seen in table 8. This table shows the value for the thermodiffusion coefficient measured using the TGC technique for two of the components of the ternary mixtures (Tol and nC$_6$). This table also contains the values for these coefficients determined by the correlation derived by Blanco *et al.* [35]. In this correlation (eq. (8)), the values of the thermodiffusion coefficients of the components of the ternary mixtures are calculated using the data of the dynamic viscosity and thermal expansion coefficient of the ternary mixture (table 4) and the data of the dynamic viscosity, thermal expansion coefficient and thermodiffusion coefficient of the corresponding binary mixtures (tables 2 and 3). In this equation the mass concentration of the components in the corresponding binary mixtures are used

$$D_T^i \frac{\nu_i}{\alpha_i} = D_T^{ij} c_i c_j \frac{\nu_{ij}}{\alpha_{ij}} + D_T^{ik} c_i c_k \frac{\nu_{ik}}{\alpha_{ik}}\,. \tag{8}$$

The obtained results show a remarkable agreement between the data obtained experimentally and the one obtained using the empirical correlation. Both results show how the denser component (toluene), goes towards the cold region, while the less dense component of the mixture (nC$_6$), migrates to the warmer zone for all concentrations investigated.

Table 8. Results Obtained for the thermodiffusion coefficient in ternary mixtures of Tol-nC$_{12}$-nC$_6$ components by the TGC technique at 298.15 K and the one obtained using the correlation by Blanco *et al.* [35] for different mass fractions.

Mass fraction			$D_T/10^{-12}\,m^2\,s^{-1}\,K^{-1}$					
c_1	c_2	c_3	Exp.		Corr. [35]		Diff. / %	
Tol	nC$_{12}$	nC$_6$	D_T^1	D_T^3	D_T^1	D_T^3	δ_1	δ_3
0.2642	0.4885	0.2471	0.58	−0.65	0.58	−0.83	0.05	−22.10
0.2413	0.6218	0.1367	0.71	−1.29	0.93	−1.41	−23.91	−8.39
0.2920	0.3272	0.3807	1.45	−1.86	1.48	−2.07	−2.46	−10.21
0.3333	0.3333	0.3333	1.45	−1.88	1.60	−1.98	−9.31	−5.27

A comparison between the obtained thermodiffusion coefficients in binary (table 5) and ternary (table 8) mixtures, shows that the thermodiffusion coefficient of the ternary mixtures is, in some cases, almost one order of magnitude smaller ($D_T \simeq 10^{-13}\,m^2\,s^{-1}\,K^{-1}$). This means that the stationary separation of the components of the mixture inside the TGC column in the case of ternary mixtures becomes smaller. In ternary mixtures the thermodiffusion coefficients have also been measured using a new thermogravitational column with the same dimensions but with double length. This leads to a strong separation of the components inside the column. In all cases the results obtained with both columns agree within the experimental error. The results given in table 8 are the mean value obtained with both columns.

Additionally, one must note the influence of the analysis method in the determination of the thermodiffusion coefficients. As it has been pointed out in ref. [58], this aspect could have influence in the values of the obtained thermodiffusion coefficients of ternary mixtures. In this case an analysis method based on the measurement of the density and the refractive index is used, which gives the possibility of analyzing the whole range of concentration of ternary mixtures with fidelity.

4 Conclusion

In this work, the transport properties at 298.15 K and 308.15 K of 14 binary mixtures composed by toluene, n-dodecane and n-hexane at different mass fractions have been determined. The measurements have been carried out using two different techniques. On the one hand the Thermal Diffusion Forced Rayleigh Scattering technique has been applied, which determined the Soret, S_T, and the molecular diffusion, D, coefficients directly, so that thermodiffusion coefficient, D_T, can be calculated. On the other hand, the Thermogravitational technique and the Sliding Symmetric Tubes techniques have been used to determine the thermodiffusion and the molecular diffusion coefficient of the mixtures, calculating then the Soret coefficient of the studied mixtures from the two different experiments. For the three coefficients analyzed, a good agreement between the experimental data obtained with the different techniques has been found, with a maximum deviation of 9%. For the system Tol-nC$_6$ we could also reproduce the literature data with the three methods.

Furthermore we investigated the correlation between the thermodiffusion coefficient and the ratio of the thermal expansion and viscosity. For most of the mixtures analyzed D_T increases as a function of the ratio (α/ν). Surprisingly we find a negative slope for the mixture Tol-nC$_6$. By comparison with measurements of benzene with short alkanes we find a similar trend. In both cases the stronger interactions of the more rigid ring compounds compared to the flexible alkanes lead to an increase of D_T with increasing content of the ring compound. And if at the same time the thermal expansion coefficient of the alkane is larger than for the ring compound we observe a decrease of D_T with α/ν, as it is observed for the short alkanes.

The study has been completed by the experimental measurement of the thermodiffusion coefficients in four ternary mixtures at 298.15 K using the thermogravitational technique. For these mixtures an analysis of the results obtained has been carried out. Additionally, three empirical correlations from the literature [35, 41, 42] have been used for the determination of the thermodiffusion and molecular diffusion coefficients in the binary and ternary mixtures. The comparison with the results obtained by the different experimental techniques leads to a good agreement in all the cases investigated. The new data for the ternary mixtures will be useful to validate and improve theoretical concepts to describe multicomponent systems.

The authors thank the financial support from Research Groups (IT557-10), GOVSORET3 (PI2011-22) and MicroSCALE of the Basque Government, TEDIBIO (DE2009-0024) of the Spanish Government and DAAD PPP program and the Deutsche Forschungsgemeinschaft grant Wi1684.

References

1. C. Ludwig, Sitz. Ber. Akad. Wiss. Wien Math.-Naturw. **20**, 539 (1856).
2. C. Soret, C.R. Acad. Sci. **91**, 289 (1880).
3. L.J. Wittenberg, in *Solar Engineering - 1985, Proceedings of the joint ASME-ASES Solar Energy Conference (Sed Seventh Annual Conference), Knoxville, Tennessee, 1985*, edited by R.B. Bannerot (The American Society of Mechanical Engineers, 1985) p. 271.
4. L. Rebai, A. Mojtabi, M. Safi, A. Mohamad, J. Sol. Energy Eng. **128**, 383 (2006).

5. F. Shehadi, M. Mseddi, M. Baccar, in *Proceedings of Thermodiffusion: Basics and Applications (IMT7), Donostia, 2006*, edited by M.M. Bou-Ali, J.K. Platten (Mondragon Uniberstsitateko zerbitzu Editoriala, 2006).
6. J. Dakyns, J. Teall, J. Geol. Soc. **48**, 104 (1892).
7. J. Teall, Nat. Sci. **4**, 288 (1892).
8. A. Grachev, J. Severinghaus, Geochim. Cosmochim. Acta **67**, 345 (2003).
9. S. Wiegand, J. Phys.: Condens. Matter **16**, R357 (2004).
10. F. Montel, Entropie **184/185**, 86 (1994).
11. F. Montel, Entropie **214**, 7 (1998).
12. F. Montel, J. Bickert, A. Lagisquet, G. Galliero, J. Pet. Sci. Technol. **58**, 391 (2007).
13. P. Baaske, C.J. Wienken, P. Reineck, S. Duhr, D. Braun, Angew. Chem., Int. Ed. **49**, 2238 (2010).
14. C.J. Wienken, P. Baaske, U. Rothbauer, D. Braun, S. Duhr, Nat. Commun. **1**, 1 (2010).
15. C. Debuschewitz, W. Köhler, Phys. Rev. Lett. **87**, 055901 (2001).
16. P. Polyakov, J. Luettmer-Strathmann, S. Wiegand, J. Phys. Chem. B **110**, 26215 (2006).
17. S. Hartmann, G. Wittko, W. Kohler, K.I. Morozov, K. Albers, G. Sadowski, Phys. Rev. Lett. **109**, 065901 (2012).
18. R. Kita, S. Wiegand, J. Luettmer Strathmann, J. Chem. Phys. **121**, 3874 (2004).
19. H. Ning, S. Wiegand, J. Chem. Phys. **125**, 221102 (2006).
20. A. Mialdun, V. Yasnou, V. Shevtsova, A. Königer, W. Köhler, D. Alonso de Mezquia, M. Bou-Ali, J. Chem. Phys. **136**, 244512 (2012).
21. H. Brenner, Phys. Rev. E **74**, 036306 (2006).
22. P. Blanco, M.M. Bou-Ali, J.K. Platten, P. Urteaga, J.A. Madariaga, C. Santamaria, J. Chem. Phys. **129**, 174504 (2008).
23. P. Blanco, S. Wiegand, J. Phys. Chem. B **114**, 2807 (2010).
24. J. Platten, M. Bou-Ali, P. Costesèque, J. Dutrieux, W. Köhler, C. Leppla, S. Wiegand, G. Wittko, Philos. Mag. **83**, 1965 (2003).
25. P. Blanco, M. Bou-Ali, J. Platten, J. Madariaga, P. Urteaga, C. Santamaría, J. Non-Equilib. Thermodyn. **32**, 309 (2007).
26. P. Blanco, P. Polyakov, M. Bou-Ali, S. Wiegand, J. Phys. Chem. B **112**, 8340 (2008).
27. G. Galliero, B. Duguay, J. Caltagirone, F. Montel, Fluid Phase Equilib. **208**, 171 (2003).
28. A. Perronace, C. Leppla, F. Leroy, B. Rousseau, S. Wiegand, J. Chem. Phys. **116**, 3718 (2002).
29. A. Leahy-Dios, A. Firoozabadi, J. Phys. Chem. B **111**, 191 (2007).
30. A. Königer, B. Meier, W. Köhler, Philos. Mag. **89**, 907 (2009).
31. S. Srinivasan, D. Alonso de Mezquia, M. Bou-Ali, M. Saghir, Philos. Mag. **91**, 4332 (2011).
32. S. Van Vaerenbergh, A. Shapiro, G. Galliero, F. Montel, J. Legros, J. Caltagirone, J. Daridon, Z. Saghir, *Multicomponent processes in crudes, European Space Agency, (Special Publication) ESA SP*, Vol. **1290** (2005) pp. 202–213.
33. K. Ghorayeb, A. Firoozabadi, SPE J. **5**, 158 (2000).
34. L. Kempers, in *Proceedings of Thermal Nonequilibrium Phenomena in Fluid Mixtures, 4th International Meeting on Thermodiffusion (IMT4), Germany, 2000*, edited by W. Köhler, S. Wiegand (Springer-Verlag, 2002).
35. P. Blanco, M. Bou-Ali, J. Platten, D. Alonso De Mezquia, J. Madariaga, C. Santamaría, J. Chem. Phys. **132**, 114506 (2010).
36. A. Königer, H. Wunderlich, W. Köhler, J. Chem. Phys. **132**, 174506 (2010).
37. A. Leahy-Dios, M. Bou-Ali, J. Platten, A. Firoozabadi, J. Chem. Phys. **122**, 234502 (2005).
38. M. Bou-Ali, J. Platten, J. Non-Equilib. Thermodyn. **30**, 385 (2005).
39. S. VanVaerenbergh, S. Srinivasan, M. Saghir, J. Chem. Phys. **131**, 114505 (2009).
40. V. Shevtsova, V. Sechenyh, A. Nepomnyashchy, J. Legros, Philos. Mag. **91**, 3498 (2011).
41. J. Madariaga, C. Santamaría, M. Bou-Ali, P. Urteaga, D. Alonso De Mezquia, J. Phys. Chem. B **114**, 6937 (2010).
42. D. Alonso de Mezquia, M. Bou-Ali, M. Larrañaga, J. Madariaga, C. Santamaría, J. Phys. Chem. B **116**, 2814 (2012).
43. W. Furry, R. Jones, L. Onsager, Phys. Rev. E **55**, 1083 (1939).
44. D. Alonso de Mezquia, F. Doumenc, M.M. Bou-Ali, J. Chem. Eng. Data **57**, 776 (2012).
45. H. Ning, R. Kita, H. Kriegs, J. Luettmer-Strathmann, S. Wiegand, J. Phys. Chem. B **110**, 10746 (2006).
46. R.D. Camerini-Otero, R.M. Franklin, L.A. Day, Biochemistry **13**, 3763 (1974).
47. V. Sechenyh, J.-C. Legros, V. Shevtsova, J. Chem. Thermodyn. **43**, 1700 (2011).
48. A.F.A. Asfour, M.H. Siddique, T.D. Vavanellos, J. Chem. Engin. Data **35**, 192 (1990).
49. A.F.A. Asfour, M.H. Siddique, T.D. Vavanellos, J. Chem. Engin. Data **35**, 199 (1990).
50. B. Gonzalez, E.J. Gonzalez, I. Dominguez, A. Dominguez, Phys. Chem. Liquids **48**, 514 (2010).
51. H. Iloukhani, M. Rezaei-Sameti, J. Basiri-Parsa, J. Chem. Thermodyn. **38**, 975 (2006).
52. G. Wittko, PhD thesis, Universität Bayreuth (2007).
53. M. M. Bou-Ali, O. Ecenarro, J. Madariaga, C. Santamaría, J. Valencia, J. Phys.: Condens. Matter **10**, 3321 (1998).
54. W. Köhler, B. Müller, J. Chem. Phys. **103**, 4367 (1995).
55. K. Zhang, M. Briggs, R. Gammon, J. Sengers, J. Chem. Phys. **104**, 6881 (1996).
56. Z. Wang, H. Kriegs, S. Wiegand, J. Phys. Chem. B **116**, 7463 (2012).
57. M. Bou-Ali, O. Ecenarro, J. Madariaga, C. Santamaria, J. Valencia, J. Non-Equilib. Thermodyn. **24**, 228 (1999).
58. A. Mialdun, V. Shevtsova, J. Chem. Phys. **138**, 161102 (2013).